

Article

Crystallography, in Silico Studies, and In Vitro Antifungal Studies of 2,4,5 Trisubstituted 1,2,3-Triazole Analogues

Katharigatta N. Venugopala ^{1,2,*}, Mohammed A. Khedr ^{1,3}, Yarabahally R. Girish ⁴, Subhrajyoti Bhandary ⁵, Deepak Chopra ⁵, Mohamed A. Morsy ^{1,6}, Bandar E. Aldhubiab ¹, Pran Kishore Deb ⁷, Mahesh Attimarad ¹, Anroop B. Nair ¹, Nagaraja Sreeharsha ^{1,8}, Rashmi V ⁹, Mahmoud Kandeel ^{10,11}, Sabah H. Akrawi ¹, Madhusudana Reddy M B ¹², Sheena Shashikanth ¹³, Osama I. Alwassil ¹⁴ and Viresh Mohanlall ²

¹ Department of Pharmaceutical Sciences, College of Clinical Pharmacy, King Faisal University, Al-Ahsa 31982, Saudi Arabia; mmohammed@kfu.edu.sa (M.A.K.); momorsy@kfu.edu.sa (M.A.M.); baldhubiab@kfu.edu.sa (B.E.A.); mattimarad@kfu.edu.sa (M.A.); anair@kfu.edu.sa (A.B.N.); sharsha@kfu.edu.sa (N.S.); sakrawi@kfu.edu.sa (S.H.A.)

² Department of Biotechnology and Food Technology, Durban University of Technology, Durban 4001, South Africa; vireshm@dut.ac.za

³ Department of Pharmaceutical Chemistry, Faculty of Pharmacy, Helwan University, Ein Helwan, Cairo 11795, Egypt

⁴ ACU-Center for Research and Innovations, BGSIT Campus, Adichunchanagiri University, B.G. Nagara, Mandya District 571448, India; girish.yr@gmail.com

⁵ Department of Chemistry, Indian Institute of Science Education and Research Bhopal, Bhopal By-pass Road, Bhauri, Bhopal 462066, India; bhandarysj@gmail.com (S.B.); dchopra@iiserb.ac.in (D.C.)

⁶ Department of Pharmacology, Faculty of Medicine, Minia University, El-Minia 61511, Egypt

⁷ Faculty of Pharmacy, Philadelphia University, Amman 19392, Jordan; prankishore1@gmail.com

⁸ Department of Pharmaceutics, Vidya Siri College of Pharmacy, Off Sarjapura Road, Bengaluru 560035, India

⁹ Department of Public health Medicine, University of KwaZulu-Natal, Howard College Campus, Durban 4041, South Africa; rashmivenugopala@gmail.com

¹⁰ Department of Biomedical Sciences, College of Veterinary Medicine, King Faisal University, Al-Ahsa 31982, Saudi Arabia; mkandeel@kfu.edu.sa

¹¹ Department of Pharmacology, Faculty of Veterinary Medicine, Kafrelsheikh University, Kafrelsheikh 33516, Egypt

¹² Department of Chemistry, School of Applied Sciences, REVA University, Bangalore 560064, India; mbmsreddy@gmail.com

¹³ Department of Studies in Organic Chemistry, University of Mysore, Manasagangotri, Mysore 570006, India; shashikanth@chemistry.uni-mysore.ac.in

¹⁴ Department of Pharmaceutical Sciences, College of Pharmacy, King Saud bin Abdulaziz University for Health Sciences, Riyadh 11481, Saudi Arabia; wassilo@ksau-hs.edu.sa

* Correspondence: kvenugopala@kfu.edu.sa; Tel.: +966-135898842

Received: 19 May 2020; Accepted: 17 June 2020; Published: 20 June 2020



Abstract: A series of 2,4,5 trisubstituted-1,2,3-triazole analogues have been screened for their antifungal activity against five fungal strains, *Candida parapsilosis*, *Candida albicans*, *Candida tropicalis*, *Aspergillus niger*, and *Trichophyton rubrum*, via a 3-[4,5-dimethylthiazol-2-yl]-2,5-diphenyltetrazolium bromide (MTT) microdilution assay. Compounds GKV10, GKV11, and GKV15 emerged as promising antifungal agents against all the fungal strains used in the current study. One of the highly active antifungal compounds, GKV10, was selected for a single-crystal X-ray diffraction analysis to unequivocally establish its molecular structure, conformation, and to understand the presence of different intermolecular interactions in its crystal lattice. A cooperative synergy of the C-H...O, C-H...N, C-H...S, C-H... π , and π ... π intermolecular interactions was present in the crystal structure, which contributed towards the overall stabilization of the lattice. A molecular docking study was

conducted for all the test compounds against *Candida albicans* lanosterol-14 α -demethylase (pdb = 5 tzl). The binding stability of the highly promising antifungal test compound, GKV15, from the series was then evaluated by molecular dynamics studies.

Keywords: 2,4,5 trisubstituted 1,2,3-triazoles; antifungal activity; single-crystal X-ray diffraction; minimum inhibitory concentration; molecular docking; dynamic studies

1. Introduction

Fungi are organisms with similar properties to plants [1]. Many fungal infections may be superficial or systematic, such as candidiasis, aspergillosis, and dermatophytosis [2]. Some diseases can increase the incidence of fungal infections, such as cancer, human immunodeficiency virus, and the overuse of antibiotics [3,4]. Available antifungal drugs have many side effects and lack selectivity towards fungi, as they harm human cells, causing a hepatotoxic effect similar to azole antifungal agents [5]. In addition, they have poor solubility and bioavailability [6]. The development of selective and safe antifungal agents with enhanced bioavailability properties is a significant challenge for pharmaceutical companies. Lanosterol-14- α -demethylase is the enzyme responsible for the synthesis of ergosterol in fungi and is a specific component in the fungal cell membrane. The inhibition of ergosterol synthesis will cause death to the fungal cell. Hence, it is a potential selective target for antifungal azole agents [7]. In silico studies suggest that lanosterol-14- α -demethylase has a great affinity for azole moieties such as diazole, triazole, and tetrazole, to bind and coordinate to the heme found in the heme-porphyrin cofactor. To date, the reported use of triazole scaffolds in antifungal drugs has been limited. A triazole scaffold has many reported pharmacological properties, such as antiviral [8], hypoglycemic [9], anti-tubercular [10,11], antimicrobial [12,13] and antihypertensive properties [14]. In continuation to our effort to apply methods [15–19] for the development of pharmacologically active heterocyclic compounds [20–35], the current study aimed to investigate the in vitro antifungal activity of synthetic 1,3,4-trisubstituted-1,2,3-triazole analogues and to computationally evaluate their binding modes.

2. Results and Discussion

2.1. Chemistry

Synthesis of the title compounds GKV1–15 (Figure 1) was achieved by two-step chemical synthesis (Scheme 1). Characterization was achieved by FT-IR, NMR (^1H and ^{13}C), High-resolution mass spectrometry (HRMS), and selected compounds using the single-crystal X-ray method, as per an earlier study [36]. The yield of the compounds was in the range of 45–82%, and the purity of the compounds was over 99%. The title compound GKV3 was studied for single-crystal X-ray study analysis, and the intermolecular interactions were further evaluated through the molecular electrostatic potential map and Hirshfeld fingerprint analysis [37].

2.2. Crystallography

The molecular structure of the molecule GKV10 in the crystal shows that it is conformationally flexible (Figure 2). The magnitudes of the torsion angles for C8-C7-C6-N3 and N1-C5-C4-O1 are 143.5° and 145.6°, respectively. Interestingly, the torsion angle for O1-C4-C3-C2 is 174.4°, indicating planarity in the solid-state structure. This could possibly result in increased delocalization of the electron density between the carbonyl groups and the thiophene ring. The packing of molecules in the crystal shows the presence of C-H \cdots N hydrogen bonds (involving acidic H3 and N3) forming molecular chains (Figure 3). These parallel chains are translated and connected via C-H \cdots O (involving H1 and O1), C-H \cdots S (involving H15 and S1), and C-H \cdots π (involving H4 and C14) intermolecular

interactions. Centro-symmetrically related chains formed via C-H...N hydrogen bonds (involving acidic H3 and N3) are further stabilized via C-H...O interactions (involving H14 and O1) and π ... π stacking interactions at a distance of 3.901(2) Å (Figure 4). Two such consecutive pairs of dimers are again centro-symmetrically related and connected via C-H... π (involving H11 and Cg1) and C-H...N (involving H5 and N3) (Figure 4). In addition, a different C-H...N dimer (involving H13 and N1) is present in the crystalline lattice, and a pair of such dimers are stabilized further via the already present C-H...O (involving H14 and O1) and C-H... π interactions (involving H4 and C14) (Figure 5).

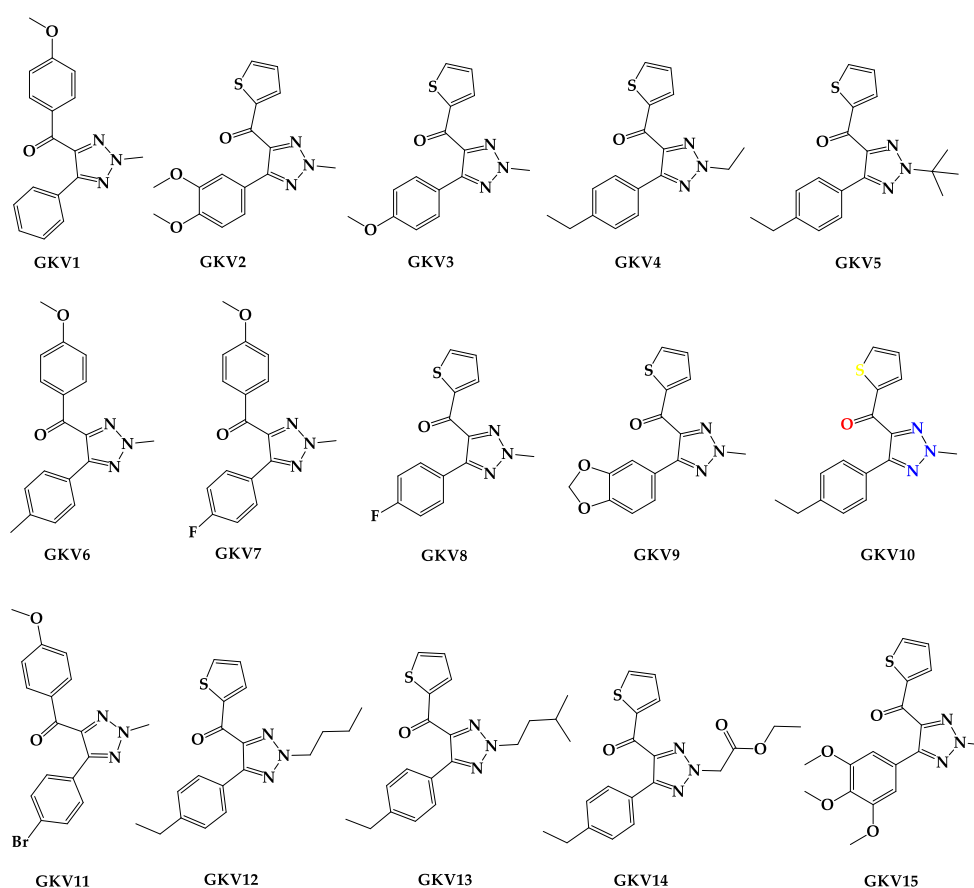
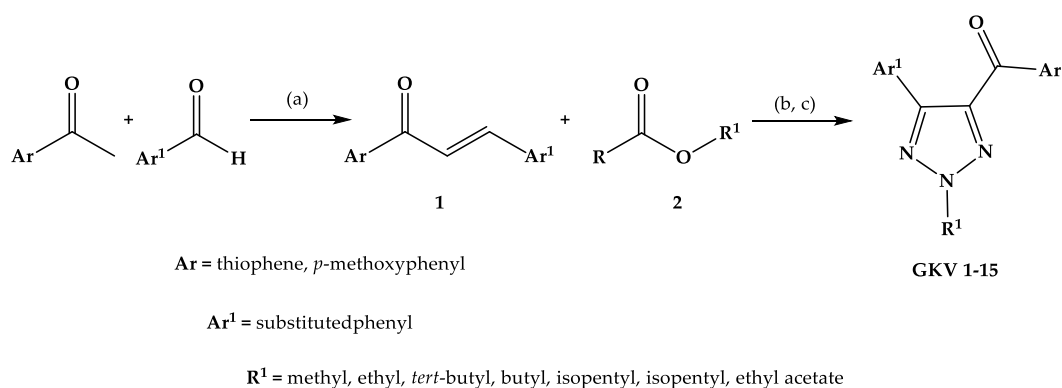


Figure 1. The molecular structures of 1,3,4-trisubstituted-1,2,3-triazole analogues (GKV1–15) studied for antifungal properties against *Candida parapsilosis*, *Candida albicans*, *Candida tropicalis*, *Aspergillus niger*, and *Trichophyton rubrum* by a 3-[4,5-dimethylthiazol-2-yl]-2,5-diphenyltetrazolium bromide (MTT) microdilution assay.



Scheme 1. Synthesis of the title compounds GKV1–15. Reagents and conditions: (a) 6N NaOH, Ethanol, 5 h, r.t; (b) NaN₃, ZrO₂-Cu₂- β -CD, DMF, 100 °C, stirred, 15 h; (c) 100 °C, stirred, 16 h.

2.3. Pharmacology

The *in vitro* antifungal minimum inhibitory concentration (MIC) was determined by using the two-fold dilution method (at 0.49, 0.98, 1.95, 3.9, 7.81, 15.63, 31.25, 62.5, and 125 $\mu\text{g/mL}$ concentrations) and the results are presented in Table 1. Compounds GKV10, GKV11, and GKV15 were selective against *Candida (C.) tropicalis* (0.49 $\mu\text{g/mL}$). They showed similar activity against *C. parapsilosis* and *C. albicans*, as well (0.98 $\mu\text{g/mL}$). Compound GKV15 had higher activity against *Aspergillus (A.) niger* and *Trichophyton (T.) rubrum* (0.98 $\mu\text{g/mL}$). The promising results of these antifungal activities may require the optimization of highly active compounds in the future.

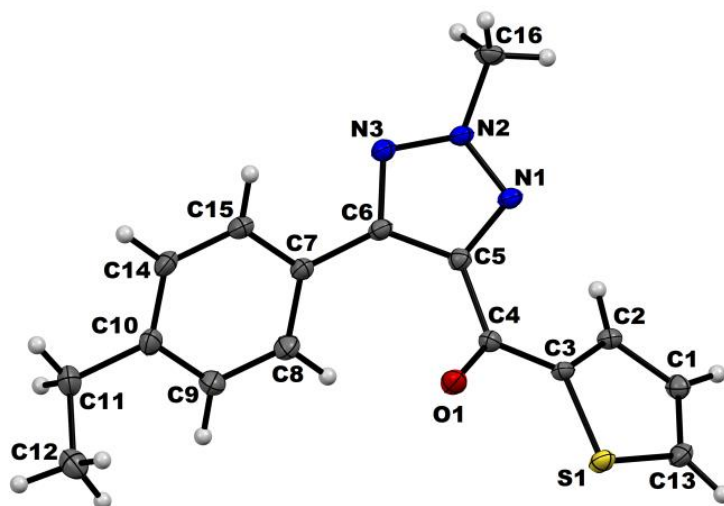


Figure 2. The Oak Ridge Thermal Ellipsoid Plot (ORTEP) of GKV10 drawn with 50% ellipsoidal probability.

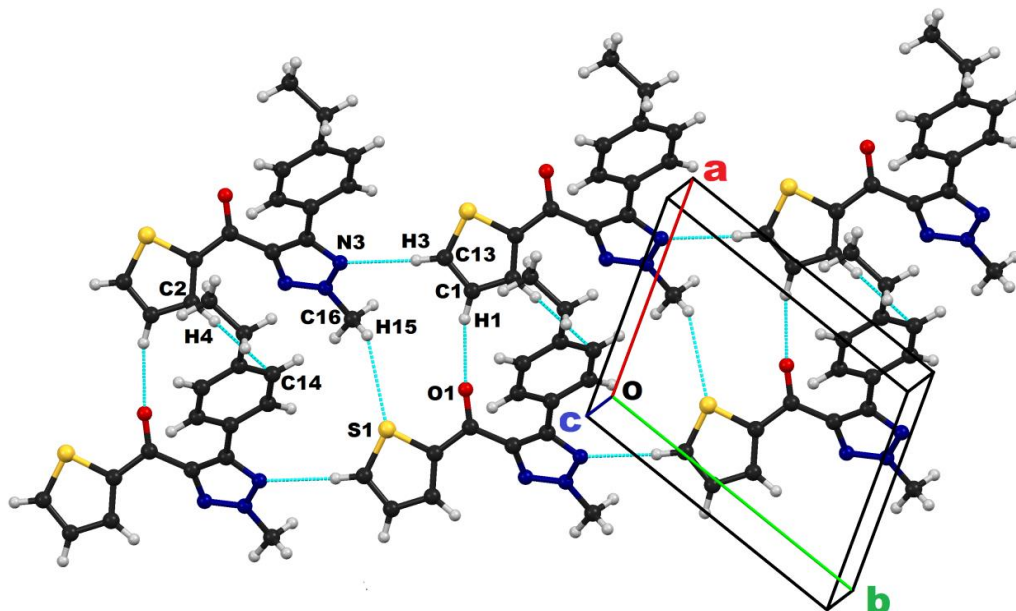


Figure 3. Packing network of molecules down the *ab* plane associated with C-H...N, C-H...O hydrogen bonds and C-H...S and C-H... π intermolecular contacts.

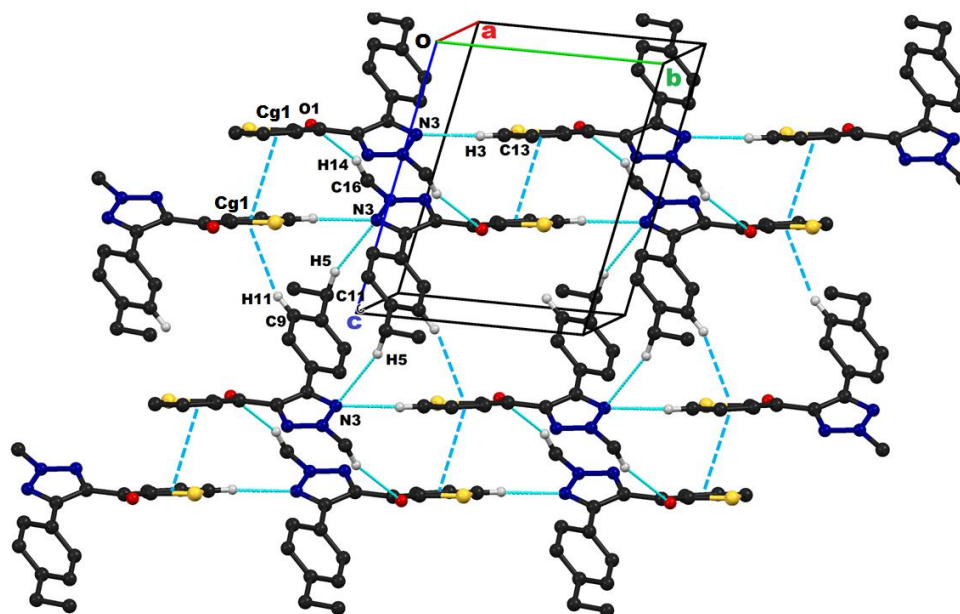


Figure 4. Packing of molecules down the *bc* plane associated with C-H...O, C-H...N, C-H...Cg1, and π ... π stacking (Cg1...Cg1) interactions. All non-interacting hydrogen atoms were removed for clarity.

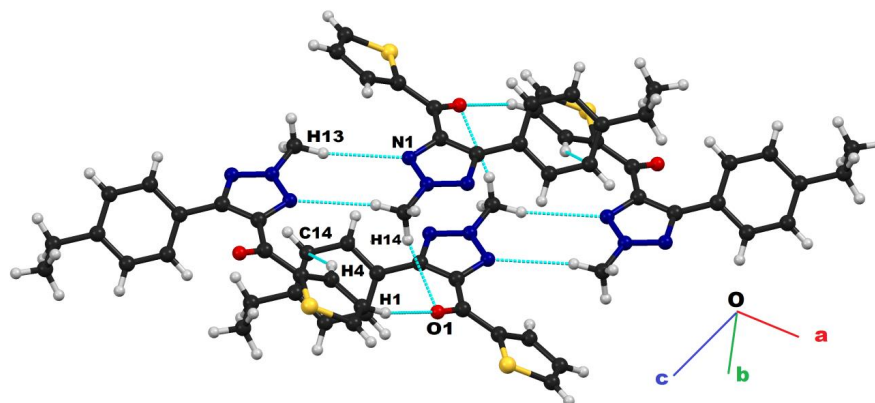


Figure 5. Centro-symmetric C-H...N dimers connected via C-H...O and C-H... π interactions.

Table 1. The antifungal activity of 5-(substituted phenyl)-2-methyl-2*H*-1,2,3-triazol-4-yl(4-substitutedphenyl/thiophenyl) methanone analogues (GKV1-15).

Compound Code	Minimum Inhibitory Concentration ($\mu\text{g/mL}$)				
	<i>C. parapsilosis</i>	<i>C. albicans</i>	<i>C. tropicalis</i>	<i>A. niger</i>	<i>T. rubrum</i>
GKV1	125	62.5	62.5	125	125
GKV2	31.25	15.63	15.63	62.5	62.5
GKV3	125	62.5	62.5	125	125
GKV4	15.63	15.63	15.63	31.25	31.25
GKV5	125	62.5	62.5	125	125
GKV6	31.5	15.63	15.63	31.25	31.25
GKV7	7.81	7.81	3.9	15.63	15.63
GKV8	7.81	7.81	3.9	15.63	15.63
GKV9	3.9	3.9	1.98	7.81	15.63
GKV10	0.98	0.98	0.49	1.95	1.95
GKV11	0.98	0.98	0.49	0.98	1.95
GKV12	15.63	15.63	15.63	31.25	31.25
GKV13	15.63	15.63	7.81	15.63	15.63
GKV14	7.81	7.81	3.9	7.81	15.63
GKV15	0.98	0.98	0.49	0.98	0.98
Fluconazole	0.49	0.49	0.98	0.49	1.95

Candida parapsilosis (ATCC RCMB 05064); *Candida albicans* (ATCC RCMB 05064); *Candida tropicalis* (ATCC RCMB 05064); *Aspergillus niger* (ATCC RCMB 05064); *Trichophyton rubrum* (ATCC RCMB 05064).

2.4. Molecular Docking

The molecular docking study was performed to evaluate the binding orientation of the tested compounds within the active site of lanosterol-14- α -demethylase. We computed scores for the free energy of binding, affinity, clash score, and the root of the mean square deviation (RMSD). Compound GKV15 showed the top-ranked ΔG value (-24.75 kcal/mol), affinity (30.01), and was the lowest in RMSD (0.81 Å) and clash score (2.25) (Table 2). Compounds GKV11, GKV10, GKV7, GKV8, and GKV9 also showed higher ΔG values of -24.54 , -24.33 , -23.98 , -23.88 , and -23.71 kcal/mol, respectively. The thiophene ring in the tested compounds contributed to the hydrophobicity required for the hydrophobic binding site. The triazole ring revealed two important roles: forming strong coordination with the heme of the heme-porphyrin complex (achieved in all of the tested compounds as shown in Figure 6) and maintaining the downward orientation of the two hydrophobic rings of the structure, which was also achieved successfully.

The length of the alkyl side chain on the *N*-atom of the triazole ring affected the binding. Presence of methyl group in compounds like GKV1-3, GKV6-11, and 15 had an electron-donating effect that enhanced the electron cloud around the nitrogen atom of the triazole ring and potentiated its coordination with the heme. However, the branching as well as increase in the carbon chain length resulted in the increase in steric hindrance, thereby effecting the coordination with the heme which probably could be the reason for detrimental effect in the activity as evident in case of the compounds 4, 5, 12, 13 and 14 (Figure 7).

2.5. Molecular Dynamics

The top-ranked compound, GKV15, with a high docking score and the best biological result was subjected to a molecular dynamics study against the standard antifungal agent, fluconazole, over 20 nanoseconds (ns) to evaluate the strength of their binding. The oscillations of the tested compound started with RMSD 1.5 Å during the first 3 ns. Then, from 3 ns to 8 ns, there were oscillations suspended between 1.25 Å and 2.00 Å. Equilibrium was reached at 2.00 Å at exactly 8 ns, which was then maintained (Figure 8). Interestingly, these oscillations were parallel to those of fluconazole, but the latter showed lower RMSD values as it reached its equilibrium at 1.5 Å.

Table 2. Molecular docking results of the (5-(substituted phenyl)-2-methyl-2*H*-1,2,3-triazol-4-yl) (4-substitutedphenyl/thiophenyl) methanone analogues of GVK1–15.

Compound	Computational Parameters			
	ΔG (kcal/mol)	Affinity	Clash Score	RMSD (Å)
GKV1	-22.64	25.88	3.50	1.11
GKV2	-22.41	25.72	3.01	1.25
GKV3	-22.94	26.32	2.95	1.03
GKV4	-22.33	26.10	3.00	1.30
GKV5	-22.04	26.34	2.84	1.25
GKV6	-22.83	24.97	2.65	1.25
GKV7	-23.98	29.45	2.33	1.01
GKV8	-23.88	29.33	2.38	0.97
GKV9	-23.71	28.95	2.35	0.94
GKV10	-24.33	29.80	2.40	0.87
GKV11	-24.54	29.87	2.51	0.85
GKV12	-21.95	25.12	3.25	1.50
GKV13	-21.67	26.74	3.13	1.61
GKV14	-22.89	25.74	2.81	1.44
GKV15	-24.75	30.01	2.25	0.81

RMSD: root of the mean square deviation.

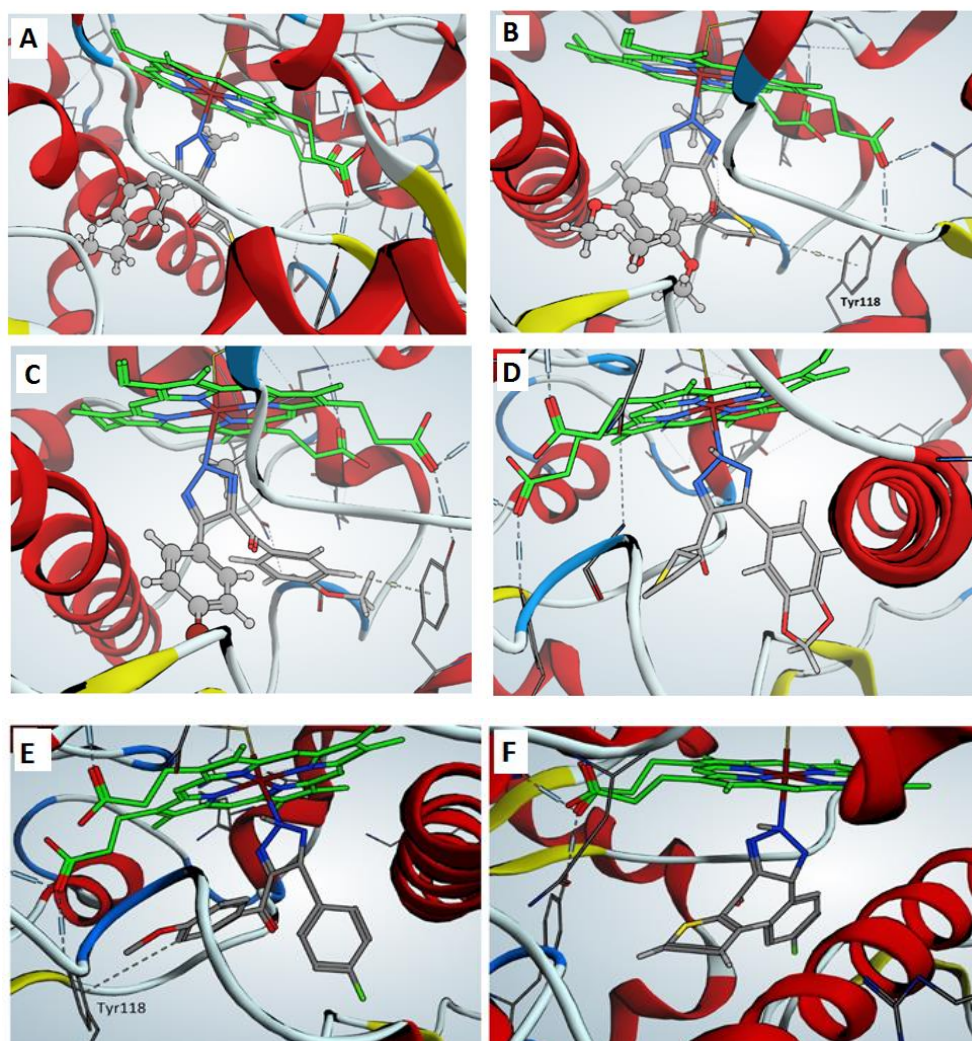


Figure 6. (A) Docking pose of the compound GKV10. (B) Docking pose of the compound GKV11. (C) Docking pose of the compound GKV15. (D) Docking pose of the compound GKV9. (E) Docking pose of the compound GKV7. (F) Docking pose of the compound GKV8.

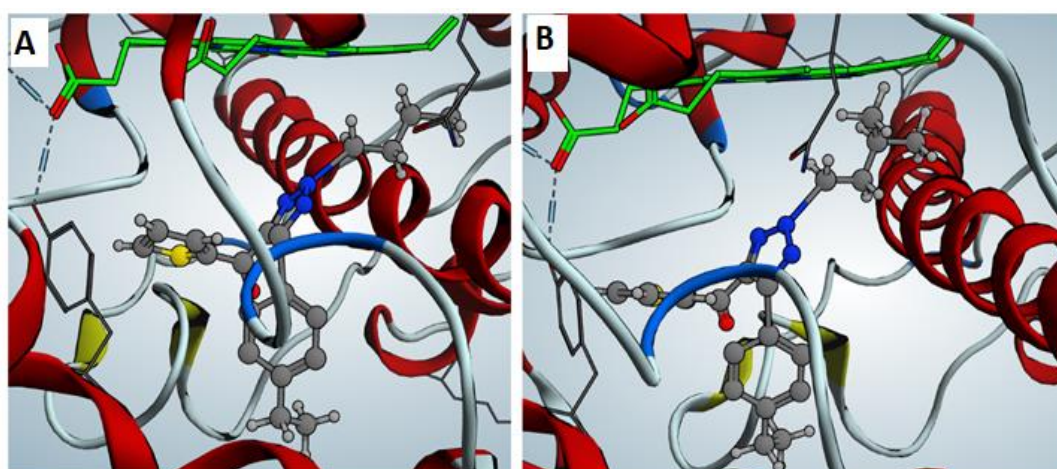


Figure 7. (A) Docking pose of compound GKV12. (B) Docking pose of compound GKV14.

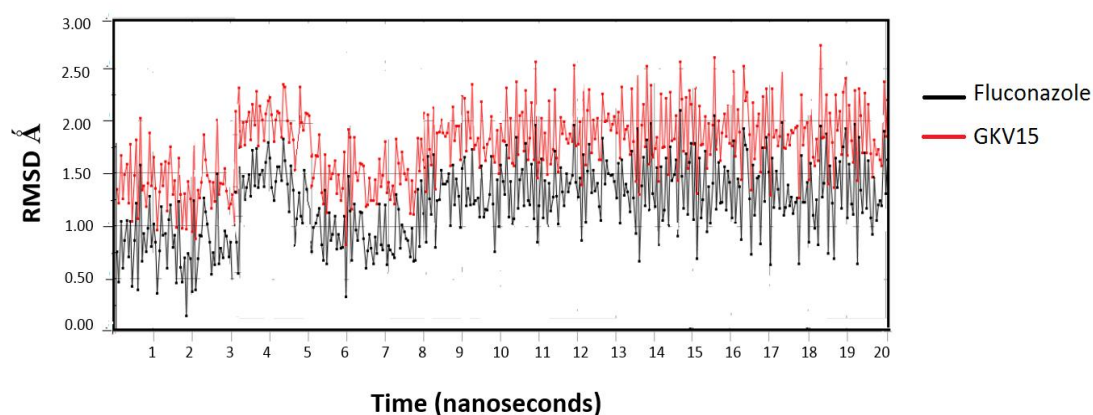


Figure 8. The molecular dynamics simulations over 20 ns.

3. Materials and Methods

3.1. General

The synthesis of the test compounds was achieved by two-step chemical synthesis and is depicted in Scheme 1, as per the previous report [36]. The molecular structures are represented in Figure 1. A single-crystal X-ray diffraction study was performed using a Bruker Kappa APEX II DUO diffractometer equipped with a charge-coupled device (CCD) detector, and monochromated Mo K α radiation ($\lambda = 0.71073 \text{ \AA}$). Data collection was carried out at 173(2) K using an Oxford Cryostream cooling system featuring the Bruker Apex II software. The in vitro antifungal test was performed at the Regional Center for Mycology and Biotechnology, Al-Azhar University, Cairo, Egypt.

3.2. Single-Crystal X-Ray Data Collection and Refinement Details

Single-crystal data were collected on a Bruker APEX II diffractometer equipped with a CCD detector, using monochromated Mo K α radiation ($\lambda = 0.71073 \text{ \AA}$). Unit cell measurement, data collection, integration, scaling, and absorption corrections for the crystal were carried out using the Bruker Apex II software [38]. Data reductions were performed with the Bruker SAINT suite [39]. The crystal structures were solved by direct methods using SIR 92 [40] and refined by the full-matrix least-squares method using SHELXL 2014 [41], which is included in the program suite WinGX (version 2014.1) [42]. Absorption corrections were applied using SADABS [43]. All non-hydrogen atoms were refined anisotropically, and all hydrogen atoms were positioned geometrically and refined using a riding model with $U_{iso}(H) = 1.2U_{eq}$. The Oak Ridge Thermal Ellipsoid Plot (ORTEP) and crystal packing diagrams were generated using the Mercury 3.5.1 (CCDC) program [44]. Geometrical calculations were performed using PARST [45] and PLATON [46]. The single-crystal data collection and refinement details are tabulated in Table 3. Intermolecular interactions involved in the title compound (5-(4-ethylphenyl)-2-methyl-2H-1,2,3-triazol-4-yl)(thiophen-2-yl)methanone (GKV10) are summarised in Table 4. Crystal information file (CIF) of compound GKV10 was deposited in The Cambridge Crystallographic Data Centre (CCDC) [47] with CCDC number 1443666 and available as electronic Supplementary Material.

3.3. Antifungal Screening

The calculation of the minimum inhibitory concentrations (MICs) for the tested compounds was done against *Candida parapsilosis* (ATCC RCMB 05064); *Candida albicans* (ATCC RCMB 05064); *Candida tropicalis* (ATCC RCMB 05064); *Aspergillus niger* (ATCC RCMB 05064); *Trichophyton rubrum* (ATCC RCMB 05064). Microdilution assay was used to evaluate the tested compounds (GKV1-15) for their antifungal activity [48]. Different concentrations were tested from each compound; 0.49, 0.98, 1.95, 3.9, 7.81, 15.63, 31.25, 62.5, and 125 $\mu\text{g/mL}$ over 48 h. The experiments were done in The Regional

Center for Mycology and Biotechnology, Al-Azhar University, Cairo, Egypt. Fluconazole was used as a reference drug.

Table 3. Single-crystal data collection and refinement.

Data	Compound GKV10
CCDC	1443666
Formula	C ₁₆ H ₁₅ N ₃ O ₃
Formula weight	297.37
Temperature/K	110 (2)
Wavelength (Å)	0.71073
Solvent system, Temperature	Toluene, 25 °C
Crystal system	Triclinic
Space group	<i>P</i> -1
<i>a</i> (Å)	7.6676 (4)
<i>b</i> (Å)	9.8450 (5)
<i>c</i> (Å)	10.8781 (6)
α (°)	94.319 (3)
β (°)	109.220 (3)
γ (°)	107.332 (3)
<i>V</i> (Å ³)	726.36 (7)
<i>Z</i> , <i>Z</i> '	1, 2
Density (g cm ⁻³)	1.360
μ (mm ⁻¹)	0.225
<i>F</i> (000)	312
θ (min, max)	2.21, 30.02
<i>h</i> _{min, max} , <i>k</i> _{min, max} , <i>l</i> _{min, max}	-10 10, -13 12, -14 14
No. of ref.	10812
No. of unique ref./obs. Ref.	3573/3098
No. parameters	172
<i>R</i> _{all} , <i>R</i> _{obs}	0.0503, 0.0442
w <i>R</i> _{all} , w <i>R</i> _{obs}	0.1301, 0.1249
$\Delta\rho$ _{min, max} (eÅ ⁻³)	-0.249, 0.446
Goodness of Fit (G. O. F.)	1.066

Table 4. Intermolecular interactions in GKV10: Cg1 refers to the center of gravity of the ring formed by C1-C2-C3-S1-C13.

Motifs	D–H...A	Symmetry	Geometry		
			D...A/Å	H...A/Å	<D–H...A/°
I	C1–H1...O1	<i>x</i> + 1, <i>y</i> , <i>z</i>	3.235 (2)	2.18	164
II	C11–H5...N3	<i>x</i> + 1, <i>y</i> , <i>z</i>	3.750 (3)	2.71	161
III	C13–H3...N3	<i>x</i> + 1, <i>y</i> + 1, <i>z</i>	3.430 (2)	2.35	175
IV	C16–H14...O1	– <i>x</i> , – <i>y</i> , – <i>z</i> + 1	3.546 (2)	2.51	159
V	C16–H13...N1	– <i>x</i> + 1, – <i>y</i> , – <i>z</i> + 1	3.824 (3)	2.76	167
VI	C2–H4...C14(π)	<i>x</i> + 1, <i>y</i> , <i>z</i>	3.875 (2)	2.99	154
VII	Cg1...Cg1	– <i>x</i> + 1, – <i>y</i> + 1, – <i>z</i> + 1	3.901 (2)	–	–
VIII	C9–H11...Cg1	– <i>x</i> + 1, – <i>y</i> + 1, – <i>z</i> + 2	3.911 (2)	3.07	149
IX	C16–H15...S1	<i>x</i> , <i>y</i> – 1, <i>z</i>	3.790 (1)	3.08	131

3.4. Molecular Docking

The Molecular Operating Environment (MOE) program was used for performing the docking studies. The chain A was selected as the main chain, which was complexed with heme–porphyrin and a reported azole inhibitor. The amino acids within a radius of 6.5 Å were selected in the binding site. The triangle method was the main placement method. London dG was used as a rescoring method. The Merck molecular force field 94x (MMFF94x) was selected as a force field [49].

3.5. Molecular Dynamics

The docking of GKV15 revealed a stable pose that was kept in the active site. The protein geometries, electron density and temperature-related factors were tested. All hydrogens were added, and energy minimization was calculated. Any foreign solvent molecules in the system were deleted; salt atoms were then added to the system to surround the biomolecular protein–ligand complex in a spherical shape. Sodium chloride was added in a 0.1 mol/L concentration. The cell dimensions were of $81.9 \times 81.9 \times 81.9 \text{ \AA}$. The total number of molecules within the system was 18,295, 1.01 g/cm^3 . Assisted Model Building with Energy Refinement 10:Extended Hückel Theory (Amber 10:EHT) was selected as a force field. The heat was adjusted in order to increase the temperature of the system from 0–300 K, which was followed by equilibration and production for 300 ps; cooling was then initiated until 0 K was reached. The simulation was conducted over a 20 ns period of time (20,000 ps).

4. Conclusions

A series of 2,4,5-trisubstituted-1,2,3-triazole derivatives (GKV1-15) bearing a substituted phenyl moiety at the fourth position of the 1,2,3-triazole nucleus was synthesized, and the derivatives were evaluated for their antifungal activity. The single-crystal X-ray diffraction studies of compound GKV10 established that C-H \cdots O, C-H \cdots N, C-H \cdots S, C-H \cdots π , and $\pi\cdots\pi$ intermolecular interactions primarily stabilized the supramolecular packing arrangement of the molecules in the solid-state. The antifungal results indicate that all the test compounds exhibited promising antifungal effects against the tested ATCC strains. The title compound GKV15 was highly promising, as it exhibited the best antifungal activity against *C. parapsilosis*, *C. albicans*, *C. tropicalis*, *A. niger*, and *T. rubrum* at an MIC of 0.98, 0.98, 0.49, 0.98, and 0.98 $\mu\text{g/mL}$, respectively. This result was combined with the molecular docking results of free energy, affinity, clash score, and RMSD at -24.75 , 30.01 , 2.25 , and 0.81 , respectively. The activity of the test compound GKV15 was similar in magnitude to the standard drug. Thus, the test compound GKV15, reported herein, is a promising starting point for the development of an antifungal drug candidate.

Supplementary Materials: The following are available online at <http://www.mdpi.com/2079-6382/9/6/350/s1>; Supplementary data (Single crystal X-ray CIF file) for compound 5-(4-ethylphenyl)-2-methyl-2H-1,2,3-triazol-4-yl(thiophen-2-yl)methanone (GKV10) related to this article can be found as an attachment.

Author Contributions: Conceptualization, K.N.V. and M.A.K.; methodology, K.N.V., M.A.K., Y.R.G., S.B., D.C., M.A.M., M.A., A.B.N. and M.R.M.B.; software, K.N.V., M.A.K., S.B., D.C. and M.K.; validation, K.N.V., M.A.K., M.A.M., P.K.D., N.S. and S.H.A.; formal analysis, K.N.V., M.A.K., Y.R.G., S.B., D.C., B.E.A., P.K.D., M.A., N.S., M.K., S.H.A., M.R.M.B., S.S., O.I.A. and V.M.; investigation, K.N.V., M.A.K., Y.R.G., S.B., D.C., A.B.N., N.S. and O.I.A.; resources, K.N.V., M.A.K., Y.R.G., D.C., R.V. and V.M.; data curation, K.N.V., M.A.K. and D.C.; writing—original draft preparation, K.N.V., M.A.K., S.B., D.C., M.A.M., M.A., A.B.N., N.S., R.V., M.K., S.H.A., M.R.M.B., S.S., O.I.A. and V.M.; writing—review and editing, K.N.V., M.A.K., S.B., D.C., B.E.A., P.K.D., A.B.N., R.V., S.H.A., S.S., O.I.A. and V.M.; visualization, K.N.V. and M.A.K.; supervision, K.N.V.; project administration, K.N.V.; funding acquisition, K.N.V., M.A.K. and B.E.A. All authors have read and agreed to the published version of the manuscript.

Funding: This research was funded by the Deanship of Scientific Research at King Faisal University, Al-Ahsa, Saudi Arabia (Nasher Track Grant No. 186196).

Acknowledgments: The authors acknowledge the Deanship of Scientific Research at King Faisal University, Kingdom of Saudi Arabia for their financial support under Nasher Track (Grant No. 186196) and their encouragement. S.B. and D.C. thank IISER Bhopal for their infrastructure and research facilities.

Conflicts of Interest: The authors declare no conflict of interest. The funders had no role in the design of the study; in the collection, analyses, or interpretation of data; in the writing of the manuscript, or in the decision to publish the results.

References

1. Panackal, A.A.; Williamson, P.R. Fungal Infections of the Central Nervous System. *Contin. Lifelong Learn. Neurol.* **2015**, *21*, 1662–1678. [[CrossRef](#)]
2. Chakrabarti, A.; Chatterjee, S.S.; Shivaprakash, M.R. Overview of opportunistic fungal infections in India. *Nihon Ishinkin Gakkai Zasshi* **2008**, *49*, 165–172. [[CrossRef](#)] [[PubMed](#)]
3. Shankar, S.K.; Mahadevan, A.; Sundaram, C.; Sarkar, C.; Chacko, G.; Lanjewar, D.N.; Santosh, V.; Yasha, T.C.; Radhakrishnan, V.V. Pathobiology of fungal infections of the central nervous system with special reference to the Indian scenario. *Neurology* **2007**, *55*, 198–215. [[CrossRef](#)] [[PubMed](#)]
4. Chakrabarti, A.; Chatterjee, S.S.; Das, A.; Shivaprakash, M.R. Invasive aspergillosis in developing countries. *Med. Mycol.* **2011**, *49*, 35–47. [[CrossRef](#)] [[PubMed](#)]
5. Khoza, S.; Moyo, I.; Ncube, D. Comparative Hepatotoxicity of Fluconazole, Ketoconazole, Itraconazole, Terbinafine, and Griseofulvin in Rats. *J. Toxicol.* **2017**, *2017*, 6746989. [[CrossRef](#)] [[PubMed](#)]
6. Siafaka, P.I.; Üstündağ Okur, N.; Mone, M.; Giannakopoulou, S.; Er, S.; Pavlidou, E.; Karavas, E.; Bikiaris, D.N. Two Different Approaches for Oral Administration of Voriconazole Loaded Formulations: Electrospun Fibers versus β -Cyclodextrin Complexes. *Int. J. Mol. Sci.* **2016**, *17*, 282. [[CrossRef](#)]
7. Khedr, M.A. Stepwise design, synthesis, and in vitro antifungal screening of (Z)-substituted-propenoic acid derivatives with potent broad-spectrum antifungal activity. *Drug Des. Dev. Ther.* **2015**, *9*, 4501–4513. [[CrossRef](#)]
8. Paeshuyse, J.; Dallmeier, K.; Neyts, J. Ribavirin for the treatment of chronic hepatitis C virus infection: A review of the proposed mechanisms of action. *Curr. Opin. Virol.* **2011**, *1*, 590–598. [[CrossRef](#)]
9. Mhasalkar, M.Y.; Shah, M.H.; Nikam, S.T.; Anantanarayanan, K.G.; Deliwala, C.V. 4-alkyl-5-aryl-4H-1,2,4-triazole-3-thiols as hypoglycemic agents. *J. Med. Chem.* **1970**, *13*, 672–674. [[CrossRef](#)]
10. Özdemir, A.; Turan-Zitouni, G.; Asim Kaplancikli, Z.; Chevallet, P. Synthesis of some 4-arylidenamino-4H-1,2,4-triazole-3-thiols and their antituberculosis activity. *J. Enzym. Inhib. Med. Chem.* **2007**, *22*, 511–516. [[CrossRef](#)]
11. Venugopala, K.N.; Dharma Rao, G.B.; Bhandary, S.; Pillay, M.; Chopra, D.; Aldhubiab, B.E.; Attimarad, M.; Alwassil, O.I.; Harsha, S.; Mlisana, K. Design, synthesis, and characterization of (1-(4-aryl)-1H-1,2,3-triazol-4-yl)methyl, substituted phenyl-6-methyl-2-oxo-1,2,3,4-tetrahydropyrimidine-5-carboxylates against *Mycobacterium tuberculosis*. *Drug Des. Devel. Ther.* **2016**, *10*, 2681–2690. [[CrossRef](#)] [[PubMed](#)]
12. Raghu Prasad, M.; Prashanth, J.; Shilpa, K.; Pran Kishore, D. Synthesis and antibacterial activity of some novel triazolothienopyrimidines. *Chem. Pharm. Bull.* **2007**, *55*, 557–560. [[CrossRef](#)] [[PubMed](#)]
13. Jayashree, B.S.; Sahu, A.R.; Srinivasa, M.M.; Venugopala, K.N. Synthesis, characterization and determination of partition coefficient of some triazole derivatives of coumarins for their anti-microbial activity. *Asian J. Chem.* **2007**, *19*, 73–78.
14. Czarnocka-Janowicz, A.; Foks, H.; Nasal, A.; Petruszewicz, J.; Damasiewicz, B.; Radwanska, A.; Kaliszan, R. Synthesis and pharmacological activity of 5-substituted-s-triazole-3-thiols. *Pharmazie* **1991**, *46*, 109–112. [[PubMed](#)]
15. Jayashree, B.S.; Arora, S.; Venugopala, K.N. Microwave assisted synthesis of substituted coumarinyl chalcones as reaction intermediates for biologically important coumarinyl heterocycles. *Asian J. Chem.* **2008**, *20*, 1–7.
16. Chandrashekarappa, S.; Venugopala, K.N.; Nayak, S.K.M.; Gleiser, R.; García, D.A.; Kumalo, H.M.; Kulkarni, R.S.; Mahomoodally, F.M.; Venugopala, R.; Mohan, M.K.; et al. One-pot microwave assisted synthesis and structural elucidation of novel ethyl 3-substituted-7-methylindolizine-1-carboxylates with larvicidal activity against *Anopheles arabiensis*. *J. Mol. Struct.* **2018**, *1156*, 377–384. [[CrossRef](#)]
17. Rao, G.K.; Venugopala, K.N.; Pai, P.N.S. Microwave-assisted synthesis of some 6-chloro-3-[2-(substituted anilino)-1,3-thiazol-4-yl]-2H-1-benzopyran-2-ones as antibacterial agents. *Indian J. Heterocycl. Chem.* **2008**, *17*, 397–400.
18. Venugopala, K.N. Design, microwave assisted synthesis and characterization of substituted 1, 2, 4-oxadiazole analogues as promising pharmacological agents. *Asian J. Chem.* **2017**, *29*, 1767–1770. [[CrossRef](#)]
19. Raghu, P.M.; Deb, P.K. Multistep, microwave assisted, solvent free synthesis and antibacterial activity of 6-substituted-2,3,4-trihydropyrimido[1,2-c]9,10,11,12-tetrahydrobenzo[b]thieno[3,2-e]pyrimidines. *Chem. Pharm Bull.* **2007**, *55*, 776–779. [[CrossRef](#)]
20. Venugopala, K.N.; Uppar, V.; Sandeep, C.; Abdallah, H.H.; Pillay, M.; Deb, P.K.; Morsy, M.A.; Aldhubiab, B.E.; Attimarad, M.; Nair, A.B.; et al. Cytotoxicity and antimycobacterial properties of pyrrolo[1,2-a]quinoline derivatives: Molecular target identification and molecular docking studies. *Antibiotics* **2020**, *9*, 233. [[CrossRef](#)]

21. Venugopala, K.N.; Tratratt, C.; Pillay, M.; Chandrashekarappa, S.; Al-Attraqchi, O.H.A.; Aldhubiab, B.E.; Attimarad, M.; Alwassil, O.I.; Nair, A.B.; Sreeharsha, N.; et al. In silico design and synthesis of tetrahydropyrimidinones and tetrahydropyrimidinethiones as potential thymidylate kinase inhibitors exerting anti-TB activity against *Mycobacterium tuberculosis*. *Drug Des. Dev. Ther.* **2020**, *14*, 1027–1039. [[CrossRef](#)] [[PubMed](#)]
22. Venugopala, K.N.; Tratratt, C.; Pillay, M.; Mahomoodally, F.M.; Bhandary, S.; Chopra, D.; Morsy, M.A.; Haroun, M.; Aldhubiab, B.E.; Attimarad, M.; et al. Anti-tubercular activity of substituted 7-methyl and 7-formylindolizines and in silico study for prospective molecular target identification. *Antibiotics* **2019**, *8*, 247. [[CrossRef](#)] [[PubMed](#)]
23. Venugopala, K.N.; Tratratt, C.; Chandrashekarappa, S.; Attimarad, M.; Sreeharsha, N.; Nair, A.B.; Pottathil, S.; Venugopala, R.; Al-Attraqchi, O.H.A.; Morsy, M.A.; et al. Anti-tubercular potency and computationally-assessed drug-likeness and toxicology of diversely substituted indolizines. *Indian J. Pharm. Edu. Res.* **2019**, *53*, 545–552. [[CrossRef](#)]
24. Venugopala, K.N.; Khedr, M.A.; Pillay, M.; Nayak, S.K.; Chandrashekarappa, S.; Aldhubiab, B.E.; Harsha, S.; Attimarad, M.; Odhav, B. Benzothiazole analogs as potential anti-TB agents: Computational input and molecular dynamics. *J. Biomol. Struct. Dyn.* **2019**, *37*, 1830–1842. [[CrossRef](#)] [[PubMed](#)]
25. Venugopala, K.N.; Chandrashekarappa, S.; Pillay, M.; Bhandary, S.; Kandeel, M.; Mahomoodally, F.M.; Morsy, M.A.; Chopra, D.; Aldhubiab, B.E.; Attimarad, M.; et al. Synthesis and structural elucidation of novel benzothiazole derivatives as anti-tubercular agents: In-silico screening for possible target identification. *Med. Chem.* **2019**, *15*, 311–326. [[CrossRef](#)]
26. Venugopala, K.N.; Sandeep, C.; Pillay, M.; Hassan, H.A.; Fawzi, M.M.; Bhandary, S.; Chopra, D.; Attimarad, M.; Bandar, E.A.; Nair, A.B.; et al. Computational, crystallographic studies, cytotoxicity and anti-tubercular activity of substituted 7-methoxy-indolizine analogues. *PLoS ONE* **2019**, *14*, e0217270. [[CrossRef](#)]
27. Chandrashekarappa, S.; Venugopala, K.N.; Venugopala, R.; Padmashali, B. Qualitative anti-tubercular activity of synthetic ethyl 7-acetyl-2-substituted-3-(4-substituted benzoyl) indolizine-1-carboxylate analogues. *J. Appl. Pharm. Sci.* **2019**, *9*, 124–128. [[CrossRef](#)]
28. Khedr, M.A.; Pillay, M.; Chandrashekarappa, S.; Chopra, D.; Aldhubiab, B.E.; Attimarad, M.; Alwassil, O.I.; Mlisana, K.; Odhav, B.; Venugopala, K.N. Molecular modeling studies and anti-TB activity of trisubstituted indolizine analogues; molecular docking and dynamic inputs. *J. Biomol. Struct. Dyn.* **2018**, *36*, 2163–2178. [[CrossRef](#)]
29. Alveera, S.; Venugopala, K.N.; Khedr, M.A.; Pillay, M.; Nwaeze, K.U.; Coovadia, Y.; Shode, F.; Odhav, B. Antimycobacterial, docking and molecular dynamic studies of pentacyclic triterpenes from *Buddleja saligna* leaves. *J. Biomol. Struct. Dyn.* **2017**, *35*, 2654–2664. [[CrossRef](#)]
30. Venugopala, K.N.; Nayak, S.K.; Pillay, M.; Prasanna, R.; Coovadia, Y.M.; Odhav, B. Synthesis and antitubercular activity of 2-(substituted phenyl/benzyl-amino)-6-(4-chlorophenyl)-5-(methoxycarbonyl)-4-methyl-3,6-dihydropyrimidin-1-ium chlorides. *Chem. Biol. Drug Des* **2013**, *81*, 219–227. [[CrossRef](#)]
31. Venugopala, K.N.; Albericio, F.; Coovadia, Y.M.; Kruger, H.G.; Maguire, G.E.M.; Pillay, M.; Govender, T. Total synthesis of a depsidomycin analogue by convergent solid-phase peptide synthesis and macrolactonization strategy for antitubercular activity. *J. Pept. Sci* **2011**, *17*, 683–689. [[CrossRef](#)]
32. Morsy, M.A.; Ali, E.M.; Kandeel, M.; Venugopala, K.N.; Nair, A.B.; Greish, K.; El-Daly, M. Screening and molecular docking of novel benzothiazole derivatives as potential antimicrobial agents. *Antibiotics* **2020**, *9*, 221. [[CrossRef](#)] [[PubMed](#)]
33. Rai, N.P.; Venugopala, K.N.; Sheena, S.; Pirama, N.A. Synthesis, characterization and anti-bacterial activity of 2-[1-(5-chloro-2-methoxy-phenyl)-5-methyl-1H-pyrazol-4-yl]-5-(substituted-phenyl)-[1,3,4] oxadiazoles. *Eur. J. Med. Chem.* **2009**, *44*, 4522–4527. [[CrossRef](#)] [[PubMed](#)]
34. Venugopala, K.N.; Jayashree, B.S. Microwave-induced synthesis of Schiff bases of aminothiazolyl bromocoumarins as antibacterials. *Indian J. Pharm. Sci.* **2008**, *70*, 88–91. [[CrossRef](#)]
35. Rai, N.P.; Narayanaswamy, V.K.; Govender, T.; Manuprasad, B.K.; Shashikanth, S.; Arunachalam, P.N. Design, synthesis, characterization, and antibacterial activity of [35]-(phenyl)-methanones. *Eur. J. Med. Chem.* **2010**, *45*, 2677–2682. [[CrossRef](#)]
36. Girish, Y.R.; Sharath Kumar, K.S.; Muddegowda, U.; Lokanath, N.K.; Rangappa, K.S.; Shashikanth, S. ZrO₂-supported Cu(ii)-[small beta]-cyclodextrin complex: Construction of 2,4,5-trisubstituted-1,2,3-triazoles via azide-chalcone oxidative cycloaddition and post-triazole alkylation. *RSC Adv.* **2014**, *4*, 55800–55806. [[CrossRef](#)]
37. Bhandary, S.; Girish, Y.R.; Venugopala, K.N.; Deepak, C. Crystal structure analysis of [5-(4-methoxyphenyl)-2-methyl-2H-1,2,3-triazol-4-yl](thiophen-2-yl)-methanone. *Acta Cryst. E* **2018**, *74*, 1178–1181. [[CrossRef](#)]

38. *Apex2, Version 2 User Manual, M86-E01078*; Bruker Analytical X-ray Systems: Madison, WI, USA, 2006.
39. Siemens. *SMART System*; Siemens Analytical X-ray Instruments Inc.: Madison, MI, USA, 1995.
40. Altomare, A.; Cascarano, G.; Giacovazzo, C.; Guagliardi, A.; Burla, M.C.; Polidori, G.; Camalli, M. SIRPOW.92—a program for automatic solution of crystal structures by direct methods optimized for powder data. *J. Appl. Crystallogr.* **1994**, *27*, 435–436. [[CrossRef](#)]
41. Sheldrick, G. A short history of SHELX. *Acta Crystallogr. Sect. A* **2008**, *64*, 112–122. [[CrossRef](#)]
42. Farrugia, L. WinGX suite for small-molecule single-crystal crystallography. *J. Appl. Crystallogr.* **1999**, *32*, 837–838. [[CrossRef](#)]
43. Sheldrick, G.M. *SADABS*; Bruker AXS, Inc.: Madison, WI, USA, 2007.
44. Macrae, C.F.; Bruno, I.J.; Chisholm, J.A.; Edgington, P.R.; McCabe, P.; Pidcock, E.; Rodriguez-Monge, L.; Taylor, R.; Van de Streek, J.; Wood, P.A. Mercury CSD 2.0—new features for the visualization and investigation of crystal structures. *J. Appl. Crystallogr.* **2008**, *41*, 466–470. [[CrossRef](#)]
45. Nardelli, M. PARST95—an update to PARST: A system of Fortran routines for calculating molecular structure parameters from the results of crystal structure analyses. *J. Appl. Crystallogr.* **1995**, *28*, 659. [[CrossRef](#)]
46. Spek, A. Structure validation in chemical crystallography. *Acta Crystallogr. Sect. D* **2009**, *65*, 148–155. [[CrossRef](#)]
47. Cambridge Crystallographic Data Centre. Available online: <https://www.Ccdc.Cam.Ac.Uk> (accessed on 28 December 2019).
48. Anaissie, E.J.; Paetznick, V.L.; Ensign, L.G.; Espinel-Ingroff, A.; Galgiani, J.N.; Hitchcock, C.A.; LaRocco, M.; Patterson, T.; Pfaller, M.A.; Rex, J.H.; et al. Microdilution antifungal susceptibility testing of *Candida albicans* and *Cryptococcus neoformans* with and without agitation: An eight-center collaborative study. *Antimicrob. Agents Chemother.* **1996**, *40*, 2387–2391. [[CrossRef](#)] [[PubMed](#)]
49. Deb, P.K.; Al-Attraqchi, O.; Mohammed, N.A.Q.; Raghuprasad, M.; Tekade, R.K. *Chapter-19: Applications of Computers in Pharmaceutical Product Formulation*; Dosage form design considerations: Advances in pharmaceutical product development and research series, Vol. II. Tekade, R.K., Ed.; Academic Press: London, UK, 2018; pp. 665–703.



© 2020 by the authors. Licensee MDPI, Basel, Switzerland. This article is an open access article distributed under the terms and conditions of the Creative Commons Attribution (CC BY) license (<http://creativecommons.org/licenses/by/4.0/>).